*cells*

MDPI

*Article*

# Negative Allosteric Modulation of Agonist-Induced $M_2$ Muscarinic Receptor/β-Arrestin Interaction by Serum Autoantibodies from Patients with Chronic Chagas Disease

**Laura C. Carrera Páez [1,†], Sabrina P. Beltrame [1,†], Sergio R. Auger [2], Ahmad H. Sabra [2], Claudio R. Bilder [3], Isabel M. Irurzun [4], Claudia I. Waldner [5] and Juan C. Goin [1,*]**

1 Laboratorio de Farmacología Molecular, Centro de Estudios Farmacológicos y Botánicos (CEFYBO-CONICET-UBA) y II Cátedra de Farmacología, Facultad de Medicina, Universidad de Buenos Aires, Buenos Aires C1121ABG, Argentina; lcarrerapaez@chu-besancon.fr (L.C.C.P.); beltri12@yahoo.com.ar (S.P.B.)
2 Hospital Donación Francisco Santojanni, Buenos Aires C1408INH, Argentina; sergioauger@aol.com (S.R.A.); amsabra@intramed.net (A.H.S.)
3 Laboratorio de Neurogastroenterología, Fundación Favaloro-Hospital Universitario, Buenos Aires C1093AAS, Argentina; cbilder@ffavaloro.org
4 Centro de Simulación Computacional para Aplicaciones Tecnológicas (CSC-CONICET), Buenos Aires C1425FQD, Argentina; i_irurzun@hotmail.com
5 Laboratorio de Inmunidad Celular y Molecular, Centro de Estudios Farmacológicos y Botánicos (CEFYBO-CONICET-UBA), Facultad de Medicina, Universidad de Buenos Aires, Buenos Aires C1121ABG, Argentina; claudiawaldner@conicet.gov.ar
* Correspondence: jcgoin@conicet.gov.ar; Tel.: +54-11-5285-3593
† These authors contributed equally to this work.

## Highlights

### What are the main findings?

- Circulating autoantibodies to $M_2$ muscarinic receptors from patients with chronic Chagas disease can inhibit the interaction of agonist-induced arrestin-2, but not arrestin-3.
- These antibodies can act as negative allosteric modulators of agonist efficacy.

### What are the implications of the main finding?

- Allosteric inhibition of agonist-induced $M_2$ receptor activation by autoantibodies could play a pathogenic role in cardiac parasympathetic dysfunction secondary to Chagas disease. These results support the potential therapeutic use of allosteric ligands to treat pathogenic effects of functional autoantibodies to $M_2$ muscarinic receptors in patients with chronic Chagas disease and other pathological conditions.

## Abstract

Inhibition of agonist-induced $M_2$ muscarinic receptor ($M_2R$) activation by functional anti-$M_2R$ autoantibodies has been associated with cardiac parasympathetic dysfunction in patients with chronic Chagas disease (CD). This study explored the allosteric nature of that inhibitory effect by assessing the ability of serum IgG from patients with CD and dysautonomia (DCD IgG) to modulate the interaction between $M_2R$ and β-arrestins in HEK 293T cells using bioluminescence resonance energy transfer. DCD IgG alone did not stimulate arrestin-2 or arrestin-3 recruitment. When cells were preincubated with DCD IgG and then treated with carbachol, arrestin-2 translocation decreased in a concentration-dependent manner, while arrestin-3 recruitment remained unaffected. Inhibition curve analysis showed a submaximal inhibitory effect (68.1 ± 2.4%) and a Hill slope less than −1 (−4.03 ± 0.39). Carbachol concentration–response assays after preincubation with DCD IgG revealed a noncompetitive inhibition of arrestin-2 recruitment, with no change in arrestin-3

check for updates

Academic Editor: Ethan Shevach

Received: 4 September 2025
Revised: 13 November 2025
Accepted: 19 November 2025
Published: 25 November 2025

**Citation:** Carrera Páez, L.C.; Beltrame, S.P.; Auger, S.R.; Sabra, A.H.; Bilder, C.R.; Irurzun, I.M.; Waldner, C.I.; Goin, J.C. Negative Allosteric Modulation of Agonist-Induced $M_2$ Muscarinic Receptor/β-Arrestin Interaction by Serum Autoantibodies from Patients with Chronic Chagas Disease. *Cells* **2025**, *14*, 1857. https://doi.org/10.3390/cells14231857

**Copyright:** © 2025 by the authors. Licensee MDPI, Basel, Switzerland. This article is an open access article distributed under the terms and conditions of the Creative Commons Attribution (CC BY) license (https://creativecommons.org/licenses/by/4.0/).

translocation. Unlikely, simultaneous exposure to DCD IgG and carbachol potentiated agonist-induced Arr-2 recruitment. We conclude that anti-$M_2R$ autoantibodies selectively inhibit agonist-induced arrestin-2 recruitment, acting as negative allosteric modulators of agonist efficacy. The direction of autoantibody-induced allosteric modulation depends on the timing of IgG application relative to the agonist and the duration of receptor exposure to autoantibodies.

**Keywords:** neglected tropical disease; *Trypanosoma cruzi*; autoimmunity; neurotransmitter receptor; signal transduction; biased ligand; dysautonomia; heart disease; pathophysiology; BRET

## 1. Introduction

Chagas disease (CD) is a neglected tropical parasitic disease caused by the protozoan *Trypanosoma cruzi* (*T. cruzi*). The infection primarily occurs in endemic areas of Latin America but spreads to other non-endemic countries in the Americas and worldwide due to the migration of infected individuals [1]. The course of CD comprises a brief acute phase characterized by high parasitemia and usually mild, nonspecific symptoms, and a chronic phase with low or undetectable parasitemia and high levels of circulating anti-*T. cruzi* antibodies. While most infected individuals remain asymptomatic for life, around 30% of them experience cardiac disorders such as conduction abnormalities, arrhythmias, dilated cardiomyopathy, or heart failure, among other complications. Besides, less than 10% of all infected patients suffer from digestive disorders, and under 5% develop neurological forms of the disease [2].

Functional autoantibodies (AAb) against $\beta_1$ and $\beta_2$ adrenergic receptors ($\beta_1$AR/$\beta_2$AR) [3–5] and $M_2$ muscarinic acetylcholine receptors ($M_2$R) have been identified in patients with chronic CD. The interaction of these antibodies with their main epitopes at the second extracellular loop (II-ECL) of their corresponding receptors promotes receptor activation and triggers receptor-specific G protein-mediated signal transduction. The main epitopes from $\beta_1$AR and $M_2$R recognized by functional AAb share structural similarities with *T. cruzi* ribosomal proteins. Hence, these AAb are believed to be the result of an autoimmune response against the parasite through a molecular mimicry mechanism [6–8].

Anti-βAR AAb are highly prevalent in patients with chronic CD and ventricular tachycardia [9], while anti-$M_2$R AAb correlate with sinus node dysfunction [9], esophageal achalasia [10], megacolon [11], and increased ventricular repolarization heterogeneity [12]. In addition, a strong association between $M_2$ muscarinic AAb and cardiac dysautonomia has been reported in asymptomatic or symptomatic individuals with CD [13]. Moreover, the levels of serum anti-$M_2$R AAb correlate with the degree of parasympathetic impairment as determined by reduced high-frequency power in heart rate variability [14]. These results suggest that these AAb could be used as diagnostic biomarkers for parasympathetic dysautonomia in CD.

Due to growing evidence suggesting that anti-$M_2$R AAb may be involved in the pathophysiology of cardiac parasympathetic inhibition, we hypothesized that these AAb could impair acetylcholine (ACh)-mediated signaling transduction by attenuating $M_2$R activation. Accordingly, we found that exposure of $M_2$R expressed in HEK 293T cells to anti-$M_2$R AAb, followed by the addition of carbachol, promotes the inhibition of agonist-induced Gi protein activation and arrestin-2 (Arr-2) recruitment to the $M_2$R [15].

As regards the mechanism underlying the inhibitory effect of anti-$M_2$R AAb on agonist-induced $M_2$R activation, most previous reports suggest that these AAb cannot promote $M_2$R desensitization or internalization [15–17]. Thus, the inhibitory effect of

anti-$M_2$R is unlikely to be the result of short-term receptor regulation. Alternatively, several studies support the notion that an allosteric mechanism could mediate this effect: (a) The II-ECL of the $M_2$R, which interacts with anti-$M_2$R AAb, contributes to the common allosteric binding site for muscarinic allosteric ligands. This means that muscarinic AAb interact with the main allosteric site of the $M_2$R [18]; (b) Anti-$M_2$R AAb exert a non-competitive inhibition of muscarinic antagonist binding to the $M_2$R, which is consistent with an allosteric antibody/receptor interaction [5,19]; (c) Anti-$M_2$R AAb enhance $M_2$ muscarinic receptor/receptor interaction through receptor crosslinking. The fact that the negative allosteric modulator (NAM) gallamine attenuates this effect suggests that gallamine competes with muscarinic AAb for binding to the receptor's allosteric binding site [20].

The data discussed above are consistent with the potential allosteric nature of the inhibitory effect of anti-$M_2$R AAb on agonist-induced $M_2$R activation. However, this hypothesis appears to contradict previous results reported by Hernández et al., who demonstrated that serum AAb from patients with CD can enhance ACh-induced negative chronotropism in isolated rabbit hearts, suggesting that anti-$M_2$R AAb can function as positive allosteric modulators (PAM) [17].

The general aim of our research was to elucidate the pharmacological basis for the role of anti-$M_2$R AAb in cardiac parasympathetic inhibition secondary to CD. Accordingly, we hypothesized that the impairment of agonist-induced $M_2$R activation by such antibodies is mediated by negative allosteric modulation. In this study, the allosteric nature of the inhibitory effect of muscarinic AAb from patients with CD on agonist-induced β-arrestin recruitment to the $M_2$R was examined in heterologous HEK 293T cells by bioluminescence resonance energy transfer (BRET). In addition, both the mode of allosteric inhibition and the ability of these AAb to act as PAM were explored. Finally, the pharmacological implications of our findings in the context of the pathophysiology of cardiac CD were addressed.

## 2. Materials and Methods

### *2.1. Patients*

Patients with chronic *T. cruzi* infection (CD) and healthy noninfected individuals were recruited at Donación Francisco Santojanni Hospital (Buenos Aires, Argentina) upon referral from the hospital outpatient clinics. All volunteers resided in the Buenos Aires Metropolitan Area at the time of the study. However, those with *T. cruzi* infection had a history of previous residence in an endemic area for CD, at least 15 years before migrating to non-endemic areas. Diagnosis of CD was based on the detection of anti-*T. cruzi* antibodies in at least two standard tests using different antigens [indirect hemagglutination (IHA) and ELISA]. In the event of a discrepancy between the two results, a third test was performed [chemiluminescence microparticle immune assay (CMIA)]. This diagnostic strategy is based on the guidelines issued by the Pan American Health Organization in 2019 [21]. All volunteers participating in the study underwent comprehensive clinical and cardiovascular assessments, including a clinical history, physical examination, a standard 12-lead electrocardiogram (ECG), a 24 h Holter ECG, and 2D echocardiography.

Volunteers with chronic systemic diseases, any other infectious diseases, or those undergoing treatment with benznidazole were excluded from participation in this study. Patients who had received an organ transplant or blood transfusions were also excluded. *T. cruzi*-infected patients exhibited ECG disturbances like conduction abnormalities or arrhythmias typical of CD [16]. However, echocardiographic features, such as left ventricular dimension, global or regional wall motion, and left ventricular ejection fraction, ranged within normal values. The ability of the autonomic nervous system to regulate blood pressure and heart rate was assessed in all patients using a set of four classical tests

(Valsalva maneuver and tilting, hyperventilation, and coughing tests) [22]. The diagnosis of dysautonomia in each patient was established based on at least two abnormal tests, according to standard procedures [23]. For our research, all volunteers were divided into two groups: Group 1: Patients with chronic CD and dysautonomia (DCD patients; $n$ = 15), and Group 2: Control noninfected individuals (Control; $n$ = 15). All DCD patients exhibited lower Valsalva ratios than age-matched normal values (cut-off value = 1.5), which has been associated with impaired parasympathetic modulation [23].

### 2.2. Reagents and Antibodies

Tetracycline hydrochloride, ampicillin sodium salt, kanamycin sulfate, Tween-20, p-nitrophenyl phosphate, tris (hydroxymethyl) aminomethane, gallamine triethiodide, atropine sulfate, carbamoylcholine chloride (carbachol), bovine serum albumin (BSA), and Folin–Ciocalteu's phenol reagent were purchased from Sigma-Aldrich (St. Louis, MO, USA). Biotechnological fetal bovine serum (FBS) was procured from Internegocios S.A. (Mercedes, Argentina). Dulbecco's modified Eagle medium with high glucose (DMEM) was purchased from Thermo Fisher Scientific (Waltham, MA, USA). Penicillin G sodium salt and streptomycin sulfate were provided by Richet Laboratories (Buenos Aires, Argentina). Diethylaminoethyl cellulose (DE-52) was purchased from Whatman (Maidstone, UK). Trypsin from bovine pancreas was purchased from Worthington (Lakewood, NJ, USA). Coelenterazine-h was obtained from Biotium (Fremont, CA, USA). Alkaline phosphatase-conjugated goat anti-human and goat anti-mouse IgG were obtained from Jackson Immuno Research (West Grove, PA, USA). The monoclonal antibody directed to the II-ECL of the human $M_2R$ (B8E5) was purchased from Novus Biologicals (Centennial, CO, USA).

### 2.3. ELISA

Sera from *T. cruzi*-infected and noninfected volunteers were tested for the presence and levels of anti-$M_2R$ Ab by indirect ELISA [24]. In this assay, a synthetic peptide within the II-ECL of the human $M_2R$ ($pM_2$) was used as an immobilized antigen. The amino acid sequence of $pM_2$ (VRTVEDGECYIQFFSNAAVTFGTAI) corresponds to residues 169–193 of the human $M_2R$ (CHRM2, Gene ID: 1129) [25]. Maxisorp microplates (Nunc, Waltham, MA, USA) were first coated with $pM_2$ (2.5 µg/well) in 0.1 M $Na_2CO_3$ buffer, pH 11, for 18 h at 4 °C and then blocked with 2% BSA in phosphate-buffered saline, pH 7.4 (PBS) for 2 h at 37 °C. Next, 100 µL of human serum diluted 1:50 in dilution buffer (1% BSA in PBS) was added to the coated wells and allowed to react with the antigen for 2 h at 37 °C. Subsequently, 100 µL of alkaline phosphatase-conjugated goat anti-human IgG diluted 1:6000 in dilution buffer was added to each well, and the plate was incubated for 1 h at 37 °C. Three washes with PBS supplemented with 1% Tween-20 were performed between incubation steps. Finally, $OD_{405nm}$ was measured after incubation with 1 mg/mL p-nitrophenyl phosphate for 30 min at room temperature. Serum immune reactivity was expressed as ELISA reactivity index (ERI), where ERI = Mean $OD_{405nm}$ of each serum sample/(Mean $OD_{405nm}$ + 2 SD of control sera) ($n$ = 15). Sera with ERI values higher than 1 (cut-off value) were taken as positive for anti-$M_2R$ AAb.

The assay included negative controls such as the blank (only substrate and stop solution), nonspecific controls with the absence of primary antibody (human serum), and sera from three patients with Chagas disease and negative immune reactivity for anti-$M_2R$ AAb as determined in a previous study [15].

As positive controls, we included six sera from patients with Chagas disease, and high ($n$ = 2), medium ($n$ = 2), and low titers ($n$ = 2) of anti-$M_2R$ AAb, as determined in a previous study [15]. In addition, we included a commercially available monoclonal antibody against the II-ECL of the human $M_2R$ ($pM_2$) with a high titer of anti-$M_2R$ AAb as detected using an

alkaline phosphatase-conjugated goat anti-mouse IgG antibody. All determinations were performed in duplicate.

### 2.4. Purification of the IgG Fraction from Human Serum

The serum IgG fractions from eight non-infected individuals seronegative for anti-$pM_2$ AAb (Control IgG), and eight *T. cruzi*-infected patients with dysautonomia seropositive for anti-$pM_2$ AAb (DCD IgG) (Mean ERI ± SEM = 2.20 ± 0.33) were purified by DEAE-cellulose chromatography, as described previously [24]. Sera were dialyzed overnight against the elution buffer (10 mM Na/K phosphate, pH 8) and then passed through DEAE-cellulose columns that had been previously equilibrated with the elution buffer. The eluted IgG peaks were concentrated by ultrafiltration (Amicon Ultrafiltration Cell, Model 8010, Millipore Corporation, Bedford, MA, USA) to approximately 10–15 mg/mL. The purity of concentrated IgG fractions was assessed by SDS-PAGE (8% T), while protein concentration in those samples was measured using the Lowry method [26].

### 2.5. Plasmids, Cell Culture, and Transfection

Several laboratories kindly provided plasmid constructs used throughout this study, as follows: $M_2$R-RLuc (Dr. N.M. Nathanson, University of Washington, Seattle, WA, USA); Arr-2-YFP and Arr-3-YFP (Dr. M. Bouvier, University of Montreal, Montreal, QC, Canada); pCEFL-GRK2 (Dr. C. Shayo, IByME-CONICET, Buenos Aires, Argentina). All recombinant plasmids were amplified in XL1blue competent cells and purified using the Wizard® Plus Maxiprep DNA Purification System (Promega, Madison, WI, USA). Human embryonic kidney cells (HEK 293T) (ATCC# CRL-3216) were provided by the American Type Culture Collection (Manassas, VA, USA). These cells were used throughout all BRET assays. These cells were cultured in Dulbecco's modified Eagle's medium (DMEM) (high glucose, 4.5 g/L) supplemented with 10% heat-inactivated FBS, 2 mM glutamine, 100 IU/mL penicillin G sodium salt, and 100 µg/mL streptomycin sulfate, and maintained at 37 °C in a humidified atmosphere with 5% $CO_2$. Transient transfections were performed on 40–50% confluent cells using a standard calcium phosphate precipitation protocol [27].

### 2.6. BRET Assays

#### 2.6.1. Preparation of Cells Expressing BRET Constructs

A cell-based BRET[1] system was used throughout this study. HEK 293T (HEKT) cells growing in 12-well plates were transiently transfected with the $M_2$ muscarinic receptor fused to *Renilla* luciferase ($M_2$R-RLuc), G protein-coupled receptor kinase 2 (GRK2), and arrestin-2 or arrestin-3 fused to the enhanced yellow fluorescence protein (Arr-2-YFP or Arr-3-YFP), yielding two alternative BRET cell systems (HEKT/Arr-2 and HEKT/Arr-3, respectively) [15,28]. After 48 h of incubation at 37 °C, cells from each well were washed twice with warm PBS and resuspended in 800 µL of a modified Krebs-Ringer-HEPES buffer (KRH) supplemented with bovine serum albumin (BSA) (KRHA: 130 mM NaCl, 5 mM KCl, 1.2 mM $MgSO_4$, 1.2 mM $CaCl_2$, 1.2 mM $Na_2HPO_4$, 10 mL glucose, 20 mM HEPES, 0·1% BSA, pH 7·4) [20].

#### 2.6.2. Assessment of Total Fluorescence, Total Luminescence, and Basal BRET Ratio

The expression of $M_2$R-RLuc and Arr-2-YFP (Arr-3-YFP) in each cell suspension was monitored by measuring total luminescence and total fluorescence, respectively. The basal BRET signal between RLuc and YFP within each BRET pair was also measured. All determinations were performed using a FLUOstar Omega multi-mode microplate reader (BMG Labtech, Ortenberg, Germany).

(a) Fluorescence determinations: Ninety microliters of each cell sample was transferred to a 96-well black-walled, clear-bottomed microplate. Ten microliters of KRHA buffer was

added to each well of the assay plate to complete a total volume of 100 µL. Total fluorescence was measured at 25 °C using an excitation filter of 485 nm and an emission filter of 535 nm.

(b) Luminescence determinations: Ninety microliters of each cell sample was transferred to a 96-well white opaque microplate. Ten microliters of a 10X coelenterazine h solution was added to each well to achieve a final substrate concentration of 5 µM. The plate was incubated at 25 °C in the dark. After 15 min of incubation, basal BRET determinations were taken by sequentially recording light intensity at 445–505 nm and 505–565 nm. Subsequently, total luminescence was measured 20 min after the addition of coelenterazine-h.

(c) Expression of results: Total fluorescence (Ft) as measured in relative fluorescence units (RFU), and total luminescence values (Lt), as measured in total luminescence units (RLU), were corrected by subtracting the background fluorescence (Fo) or background luminescence (Lo) determined in wells containing untransfected cells, respectively. As a result, corrected fluorescence (Fc) was calculated as Fc = Ft − Fo, while corrected luminescence (Lc) was calculated as Lc = Lt − Lo. The BRET ratio was calculated as BRET = $Lc_{505–565nm}/Lc_{445–505nm}$.

#### 2.6.3. BRET Protocols

Using $F_c$ and $L_c$ values from each transfected cell suspension, $F_c/L_c$ ratios were determined, and suspensions with similar $F_c/L_c$ ratios were pooled. Seventy microliters of pooled HEKT/Arr-2 or HEKT/Arr-3 cells were distributed in luminescence microplates.

Determination of Arr-2 or Arr-3 recruitment on the corresponding BRET cell system was performed at 25 °C using three different BRET procedures (a–c) [28]:

(a) To evaluate the effects of carbachol or IgG fractions on β-arrestin recruitment, cells were treated with carbachol, DCD IgG, or Control IgG for 20, 30, or 60 min.

(b) To assess the modulatory effect of muscarinic orthosteric or allosteric ligands, or IgG fractions, on agonist-induced Arr-2 or Arr-3 recruitment, cells were preincubated with atropine, gallamine, Control IgG, or DCD IgG fraction for 0, 15, 30, and/or 60 min. Then, carbachol was added, and cells were incubated for an additional 20 min.

(c) To assess the ability of a muscarinic peptide ($pM_2$) to neutralize the inhibitory effect of DCD IgG on agonist-induced Arr-2 or Arr-3 translocation, DCD IgG fractions were first incubated with the muscarinic peptide for 30 min at 37 °C. Then, cells were preincubated with DCD IgG/$pM_2$ cocktails for 30 min and further treated with carbachol for an additional 20 min.

Readings and Expression of Results (a–c): Fifteen minutes before the end of the total incubation time, 10 µL of 10X coelenterazine h solution was added to achieve a final substrate concentration of 5 µM at a final volume of 100 µL/well. Net BRET values were obtained following treatment with carbachol or IgG fractions, with or without pretreatment, and expressed as ΔBRET = (BRET ratio after treatment with carbachol or IgG fractions) − (BRET ratio after treatment with KRHA buffer alone). All ΔBRET values were multiplied by 1000 and expressed as millibrets (mB).

### *2.7. Statistical Analysis*

Stimulation and inhibition concentration response curves were analyzed by nonlinear regression using a three-parameter logistic model with variable slope. Comparison among pharmacodynamic parameters was analyzed using the extra sum-of-squares F test or one-way ANOVA, followed by Bonferroni's post hoc test. Corresponding equations, as well as suggestions for curve fitting and parameter definition, are shown in Supplementary Materials. Differences in the means of a continuous dependent variable across different groups defined by two categorical independent variables were analyzed using a two-way ANOVA, followed by Bonferroni's post hoc test.

Throughout the present study, a $p$-value of 0.05 or less was considered statistically significant. The symbols *, &, or # are used as abbreviations in figures and tables to denote different degrees of statistical significance ($p$-value thresholds), with a greater number of symbols indicating a lower, more significant $p$-value. An asterisk (*) symbol corresponds to specific $p$-value thresholds as follows: *: $p \leq 0.05$, **: $p < 0.01$, ***: $p < 0.001$, ****: $p < 0.0001$. For the ampersand (&) and hash (#) symbols, the same pattern of increasing significance with multiplicity is used. All statistical analyses were performed using the software GraphPad Prism v.8. (GraphPad, La Jolla, CA, USA).

## 3. Results

### *3.1. Agonist-Induced β-Arrestin Translocation in HEK 293T Cells. Orthosteric and Allosteric Modulation*

The main goal of this study was to assess the allosteric nature of the inhibition of agonist-induced $M_2R$/β-arrestin interaction promoted by anti-$M_2R$ AAb from DCD patients. Because the effect of these AAb on Arr-3 recruitment to the activated $M_2R$ had not been previously addressed, we first compared the abilities of Arr-2 and Arr-3 to interact with this receptor upon carbachol stimulation. In addition, the modulatory activity of these effects by orthosteric and allosteric ligands was examined.

Treatment of HEKT/Arr-2 or HEKT/Arr-3 cells with carbachol at varying concentrations resulted in concentration-dependent increases in the BRET signal between RLuc and YFP, indicating that either Arr-2 or Arr-3 is recruited to the $M_2R$ upon agonist exposure (Figure 1A,B). Comparison of pharmacodynamic parameters $E_{max}$ and $pEC_{50}$ between HEKT/Arr-2 and HEKT/Arr-3 cells using the extra sum of squares F test showed no significant differences [$E_{max}$ (mB): 29.9 ± 0.6 (Figure 1A), 30.9 ± 0.9 (Figure 1B); $pEC_{50}$: 5.85 ± 0.08 (Figure 1A), 5.78 ± 0.11 (Figure 1B)]. The fact that the efficacy and potency values of carbachol acting on both cell systems are not significantly different suggests that the translocation of Arr-2 and Arr-3 is governed by a shared mechanism (Figure 1A,B).

Subsequently, either cell system was preincubated with atropine (a muscarinic antagonist) or gallamine (a muscarinic NAM) at varying concentrations for 15 min, and further treated with carbachol at a 10 μM final concentration for an additional 20 min. Both ligands inhibited carbachol-induced translocation of either β-arrestin in a concentration-dependent manner (Figure 1C,D). In particular, atropine promoted complete inhibition of agonist-induced $M_2R$/Arr-2 or $M_2R$/Arr-3 interaction ($I_{max} \geq 100\%$) with a Hill slope close to −1, which indicates that the antagonist binds to the orthosteric site of the receptor (competitive antagonism) (Table 1). Conversely, the effects of gallamine on agonist-induced translocation of Arr-2 or Arr-3 exhibited two classical properties of NAM: a partial maximal inhibition ($I_{max} < 100\%$) ("ceiling" effect) and a Hill slope less than −1, which is consistent with a negative cooperative effect (Figure 1C,D and Table 1).

**Table 1.** Inhibition of agonist-induced β-arrestin recruitment by orthosteric and allosteric ligands. Pharmacodynamic parameters.

| | Arrestin-2 | | | Arrestin-3 | | |
|---|---|---|---|---|---|---|
| **Ligand** | **$pIC_{50}$** | **$I_{max}$ (%)** | **Hill Slope** | **$pIC_{50}$** | **$I_{max}$ (%)** | **Hill Slope** |
| Atropine | 6.83 ± 0.10 * | 108.5 ± 5.1 ** | −0.82 ± 0.12 **** | 6.94 ± 0.09 * | 109.2 ± 4.4 *** | −0.76 ± 0.09 **** |
| Gallamine | 6.16 ± 0.29 | 73.2 ± 4.9 | −0.31 ± 0.05 | 6.24 ± 0.26 | 70.9 ± 4.0 | −0.27 ± 0.03 |

Maximal Inhibitory effect ($I_{max}$), negative log of the half-maximal inhibitory concentration ($pIC_{50}$), and Hill slope values, as determined by nonlinear regression analyses of data shown in Figure 1C,D, are listed. Comparison of pharmacodynamic parameters between curves within each panel or between them was performed using the extra sum of squares F test. Data are presented as the mean ± SEM. Significant differences vs. gallamine-preincubated cells are indicated (* $p < 0.05$, ** $p < 0.01$, *** $p < 0.001$, **** $p < 0.0001$). $pIC_{50}$, $I_{max}$, and Hill slope were not significantly different between HEKT/Arr-2 and HEKT/Arr-3 cells.

As regards the orthosteric and allosteric inhibition of agonist-induced arrestin recruitment to the $M_2R$, none of the pharmacodynamic parameters ($I_{max}$, $IC_{50}$, or Hill slope) were significantly different between HEKT/Arr-2 and HEKT/Arr-3 cells. This suggests that no significant functional differences appear to exist between the two isoforms of β-arrestin.

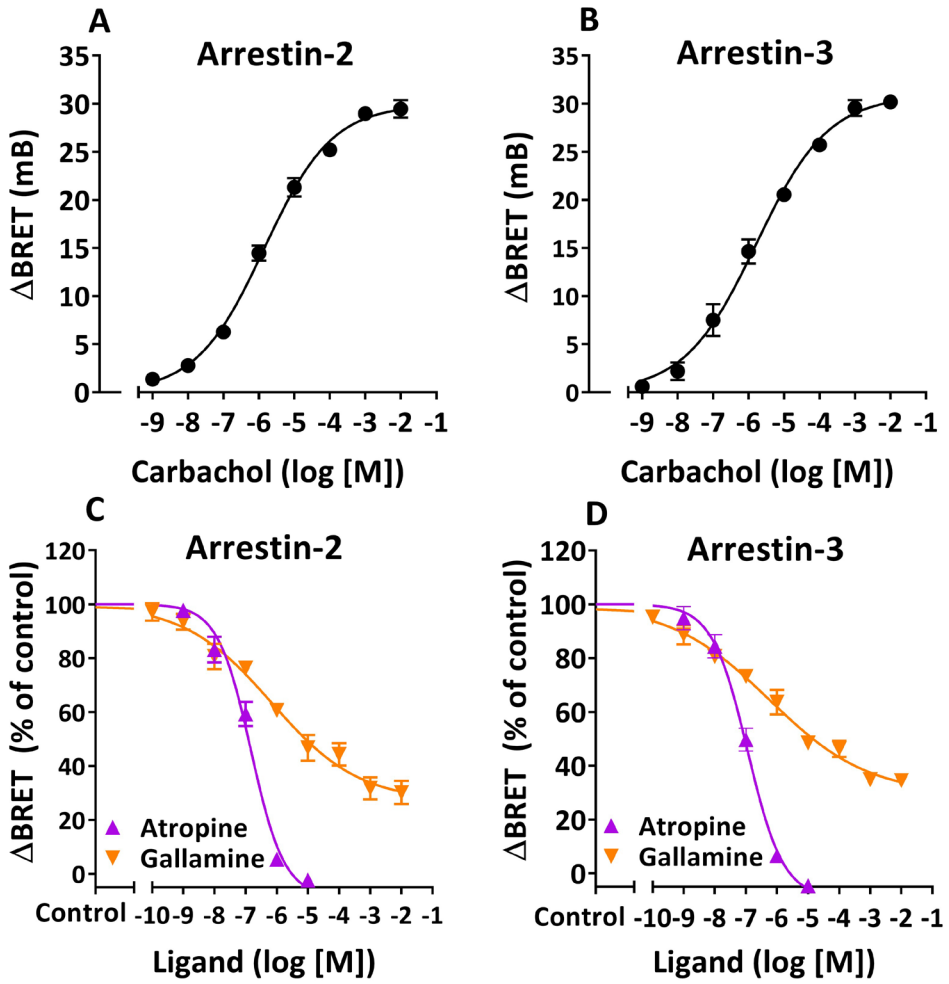



**Figure 1.** Characterization of agonist-induced β-arrestin recruitment in human cells expressing $M_2$ muscarinic receptors. Inhibition by orthosteric and allosteric ligands. HEK 293T cells expressing $M_2R$-RLuc, GRK2, and Arr-2-YFP (HEKT/Arr-2) or Arr-3-YFP (HEKT/Arr-3) were treated with carbachol at various concentrations for 20 min (**A**,**B**). Alternatively, either cell preparation (HEKT/Arr-2 or HEKT/Arr-3) was preincubated in the presence or absence of atropine or gallamine at multiple concentrations for 15 min, and then treated with carbachol (10 μM) for an additional 20 min (**C**,**D**). At the end of either procedure ((**A**)/(**B**) or (**C**)/(**D**)), BRET was determined in the presence of 5 μM coelenterazine h. Net changes in BRET were calculated as ΔBRET values and expressed in mB, where ΔBRET is the BRET ratio in the presence of agonist minus the BRET ratio in the presence of KRH buffer alone. (**A**,**B**) Data are expressed as ΔBRET (mB). (**C**,**D**) Data are expressed as a percentage of control ΔBRET values, which correspond to cells preincubated with KRH buffer alone and further treated with carbachol. Control values: 21.5 ± 0.8 mB (atropine) and 20.6 ± 1.2 mB (gallamine) (**C**); 20.5 ± 0.8 mB (atropine) and 20.2 ± 1.8 mB (gallamine) (**D**). Data shown are the mean ± SEM of four independent experiments performed at least in triplicate. All curves were best fit to a sigmoidal function using nonlinear regression analysis. Analysis of pharmacodynamic parameters derived from the data plotted in (**C**,**D**) is presented in Table 1.

### *3.2. Effect of Serum $M_2$ Muscarinic Receptor Autoantibodies on β-Arrestin Recruitment*

Before investigating whether anti-$M_2R$ AAb could modulate agonist-induced β-arrestin recruitment to the $M_2R$, the ability of these AAb to enhance $M_2R$/β-arrestin interaction

in the absence of agonist was assessed. Therefore, the effects of IgG fractions from three different DCD patients or control volunteers on the translocation of Arr-2 versus Arr-3 were compared by performing BRET assays on HEKT/Arr-2 and HEKT/Arr-3 cells. As shown in Figure 2, carbachol (10 μM) induced Arr-2 or Arr-3 translocation to the $M_2R$, as measured by an increase in the BRET signal between $M_2R$-RLuc and Arr-2-YFP (or Arr-3-YFP), which ranged from 21 to 23 mB after 30 min or 60 min of agonist treatment. In contrast, Control IgG or DCD IgG, at varying concentrations, failed to enhance the BRET signal after treatment for either 30 or 60 min. These data indicate that $M_2R$ AAb from DCD patients do not stimulate the interaction between the $M_2R$ and Arr-2 or Arr-3 in the absence of an agonist.

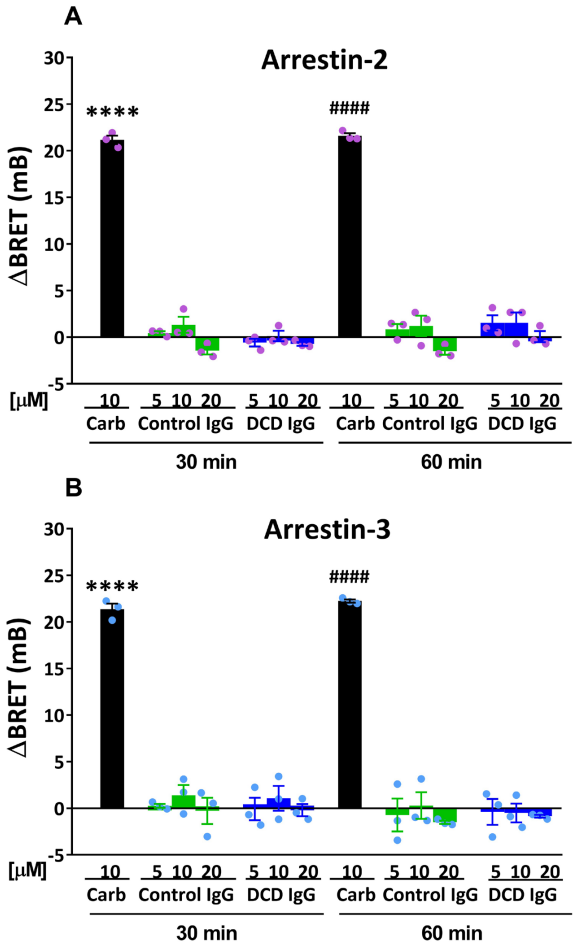



**Figure 2.** Interaction between $M_2R$ and β-arrestins in the presence of serum anti-$M_2R$ antibodies from patients with Chagas disease and dysautonomia (DCD patients). HEKT/Arr-2 (**A**) or HEKT/Arr-3 cells (**B**) were incubated with 10 μM carbachol or IgG from control individuals (Control IgG) or IgG from DCD patients (DCD IgG) at various concentrations for 30 or 60 min at 25 °C. BRET signals were determined as indicated in Figure 1. Net changes in BRET are shown as ΔBRET values and expressed in mB, where ΔBRET represents the BRET ratio in the presence of agonist or IgG fractions minus the BRET ratio in the presence of KRH buffer alone. Each bar represents the mean ± SEM of three Control or DCD IgG fractions or three experiments with carbachol performed at least in triplicate. Data were analyzed by two-way ANOVA followed by a post hoc Bonferroni test. Significant differences were observed compared to cells treated with Control or DCD IgG fractions for 30 min (**** $p < 0.0001$) (**A**) or 60 min (#### $p < 0.0001$) (**B**).

### *3.3. Allosteric Modulation of Agonist-Induced β-Arrestin Recruitment by $M_2$ Muscarinic Autoantibodies*

The abilities of IgG fractions from three different control or DCD patients to modulate agonist-induced Arr-2 vs. Arr-3 translocation to the $M_2R$ were compared using the

same BRET cell systems as before. HEKT/Arr-2 or HEKT/Arr-3 were first preincubated with Control IgG or DCD IgG at varying concentrations for 30 min and then treated with carbachol for 20 min before BRET determinations. Control IgG was unable to modulate the interaction of $M_2R$ with either Arr-2 or Arr-3 in the presence of carbachol at all concentrations tested (Figure 3A,B). In contrast, DCD IgG promoted a concentration-dependent decrease in agonist-induced Arr-2 translocation. However, the same DCD IgG fractions failed to inhibit agonist-induced Arr-3 recruitment (Figure 3A,B). Data from DCD IgG in Figure 3A were fit to a sigmoid curve using nonlinear regression analysis, which revealed pharmacodynamics parameters $I_{max}$ = 68.1 ± 2.4%, $pIC_{50}$ = 5.26 ± 0.02, and Hill slope = −4.03 ± 0.39. A submaximal inhibitory value and a Hill slope less than -1 are consistent with negative allosteric modulation. Therefore, these data suggest that anti-$M_2R$ AAb promote allosteric inhibition of agonist-induced Arr-2 recruitment to the target muscarinic receptor. Because agonist-induced $M_2R$/Arr-3 interaction is unchanged by anti-$M_2R$ AAb, we conclude that the negative allosteric modulation of agonist-induced β-arrestin recruitment is biased towards Arr-2.

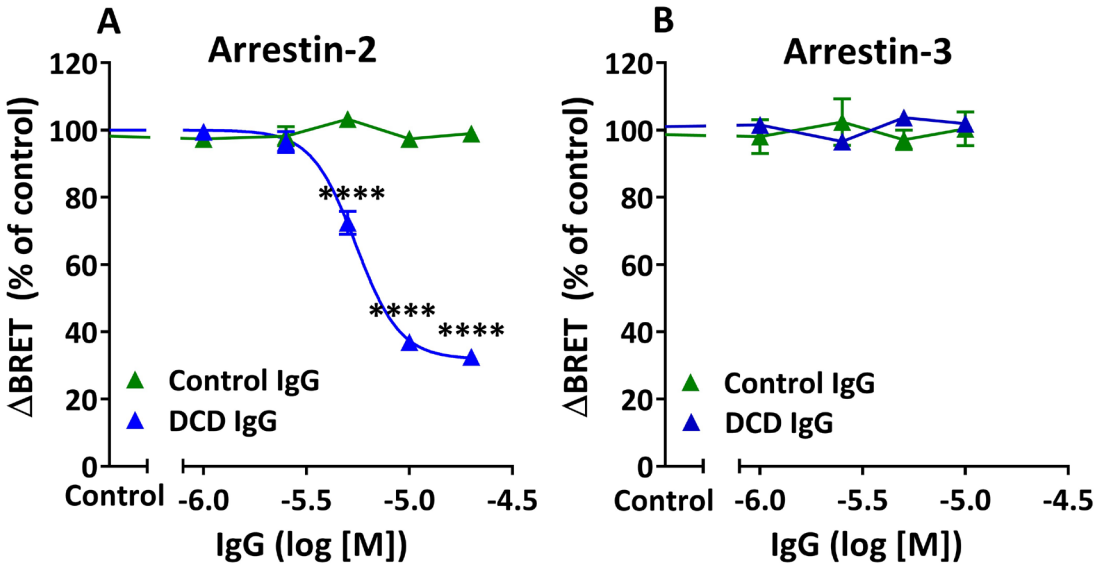



**Figure 3.** Differential effects of serum IgG anti-$M_2R$ antibodies from DCD patients on carbachol-induced β-arrestin recruitment. HEKT/Arr-2 (**A**) or HEKT/Arr-3 (**B**) cells were preincubated with Control or DCD IgG at varying concentrations for 30 min at 25 °C and then treated with carbachol (10 μM) for an additional 20 min before BRET recordings. Net changes in the BRET ratio were determined as ΔBRET and expressed in mB, as described in Figure 1. Data are shown as a percentage of control ΔBRET values, which correspond to cells treated with carbachol after preincubation with KRHA buffer alone. Data shown are the mean ± SEM of three Control or DCD IgG fractions tested in both HEKT/Arr-2 and HEKT/Arr-3 cell systems. Differences between Control and DCD IgG fractions were analyzed using two-factor ANOVA followed by a Bonferroni post hoc test. ((**A**) **** $p < 0.0001$; (**B**) NS). Data showing the effect of DCD IgG on carbachol-induced $M_2R$/Arr-2 translocation was best fit to a sigmoidal function using nonlinear regression analysis.

### *3.4. Epitope Specificity of the Negative Allosteric Modulation by $M_2$ Muscarinic Autoantibodies*

The common allosteric binding site for muscarinic allosteric ligands at the $M_2R$ involves an acidic amino acid sequence (EDGE) within the second extracellular loop (II-ECL) [18]. To demonstrate that the negative allosteric activity of DCD IgG is mediated by the interaction of AAb with the allosteric binding site of the human $M_2R$, we assessed the ability of a 25-mer peptide carrying the amino acid sequence of the II-ECL ($pM_2$) to neutralize DCD IgG-mediated inhibition of agonist-induced Arr-2 recruitment using the above-mentioned BRET assay. Preincubation of DCD IgG with increasing amounts of $pM_2$,

followed by cell treatment with DCD IgG/$pM_2$ complexes, resulted in a $pM_2$ concentration-dependent attenuation of the inhibitory activity of DCD IgG on agonist-induced Arr-2 recruitment, which reached complete neutralization of AAb-mediated inhibitory activity at [$pM_2$] = 10 μM (Figure 4). Nonlinear analysis of the data revealed pharmacodynamic parameters: Emax (101 ± 4%), $pCE_{50}$ (7.04 ± 0.16), and Hill Slope (0.91 ± 0.25). These data demonstrate that the negative allosteric activity of DCD IgG is mediated by the interaction of anti-$M_2$R AAb with the allosteric binding site of the $M_2$R.

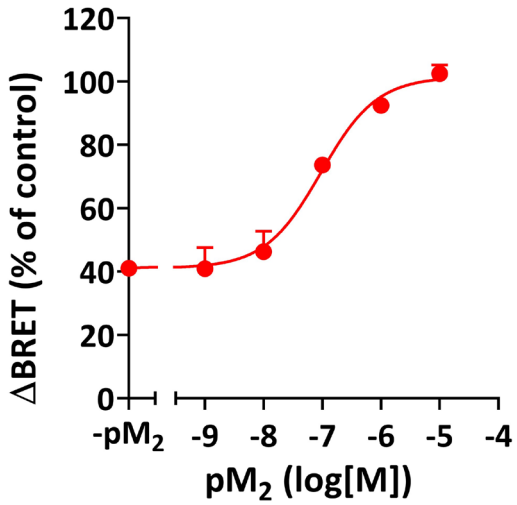



**Figure 4.** Inhibitory effect of IgG autoantibodies from DCD patients on Arr-2 recruitment to the $M_2$R. Epitope specificity. Aliquots of serum IgG fractions from DCD patients (100 μM) were mixed with the muscarinic peptide $pM_2$ at different concentrations (10 nM–100 μM) and incubated at 37 °C for 30 min. Then, HEKT/Arr-2 cells were preincubated at 25 °C for 30 min in the presence or absence of DCD IgG/$pM_2$ cocktails diluted 1:10 in KRHA buffer, and further treated with carbachol (10 μM) for an additional 20 min at the same temperature. After BRET determinations, ΔBRET values were calculated and expressed in mB, as described in Figure 1. Data are shown as a percentage of the control ΔBRET value, which corresponds to cells treated with carbachol after preincubation with KRHA buffer alone (control ΔBRET value: 23.0 ± 0.6 mB, $n$ = 3). Each data point represents the mean ± SEM of three IgG fractions from different DCD patients, performed at least in triplicate. Data were best fit to a sigmoidal function using nonlinear regression analysis.

### *3.5. Allosteric Modulation by $M_2$ Muscarinic Autoantibodies: Dependence on the Timing and Duration of Exposure of $M_2$ Muscarinic Receptors to Specific Autoantibodies*

Previous reports have shown that the simultaneous exposure of $M_2$R from an isolated heart preparation to both ACh and serum anti-$M_2$R AAb resulted in an enhanced efficacy of ACh in promoting a negative chronotropic response [17]. These findings suggest that $M_2$ muscarinic AAb behave as PAM of ACh-mediated responses. In contrast, the present study shows that the exposure of $M_2$R to anti-$M_2$R, AAb, followed by the addition of carbachol, results in an inhibition of agonist-induced Arr-2 recruitment, which suggests that these AAb can also act as NAM. Based on these results, we next examined whether the direction of allosteric modulation of agonist-induced receptor activation depends on the timing and duration of the exposure of $M_2$R to AAb using our BRET-based assay. HEKT/Arr-2 cells were preincubated with DCD IgG for 0, 15, 30, or 60 min, and further treated with 10 μM carbachol for an additional 20 min. Cells treated with a mixture of 10 μM DCD IgG and 10 μM carbachol for 20 min (preincubation time with DCD IgG = 0 min) yielded a 44.9 ± 3.1% increase in BRET as compared with those treated with 10 μM carbachol alone. However, when the duration of preincubation was gradually increased up to 60 min, a time-dependent decrease in agonist-induced Arr-2 recruitment was observed (Figure 5A). Data were best fit to an exponential one-phase decay curve with a half-life

value of 15.79 ± 0.01 min and a rate constant (K) value of 0.044 ± 0.008 $min^{-1}$ (Figure 5B). The inhibitory effect of DCD IgG was 75.4 ± 4.6% at 60 min of preincubation time. This value was not significantly different from the inhibitory effect at 30 min (61.5 ± 5.8%). Therefore, the preincubation time with human DCD IgG used throughout this study was 30 min. These data indicate that anti-$M_2$R AAb can enhance carbachol-induced Arr-2 recruitment when AAb and the muscarinic agonist act simultaneously. However, the exposure of $M_2$R to $M_2$ muscarinic AAb for at least 30 min before agonist addition results in a time-dependent inhibition of agonist-induced Arr-2 recruitment. In summary, the allosteric modulation of agonist-induced Arr-2 translocation depends on the timing and the duration of the exposure of $M_2$R to specific AAb.

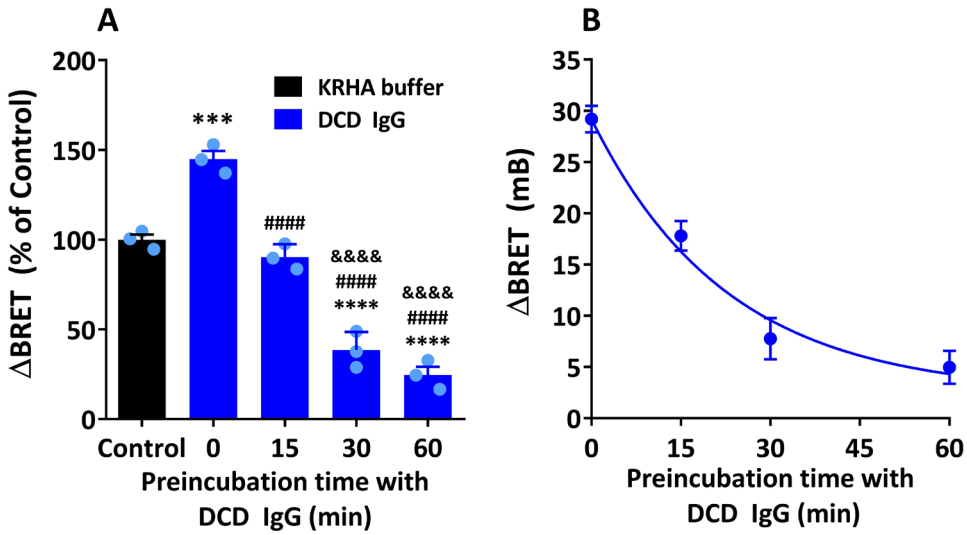



**Figure 5.** Effect of anti-$M_2$R muscarinic antibodies on agonist-induced Arr-2 recruitment. Influence of preincubation time with DCD IgG. HEKT/Arr-2 cells were preincubated with buffer alone or DCD IgG (10 μM) for 0, 15, 30, or 60 min at 25 °C. Cells were then treated with carbachol (10 μM) for an additional 20 min before BRET recordings. Net changes in the BRET ratio were calculated as ΔBRET values and expressed in mB (**B**). Alternatively, data are presented as a percentage of the control ΔBRET value, which corresponds to cells treated with carbachol after preincubation with KRHA buffer alone (**A**). Each data point represents the mean ± SEM of three IgG fractions from different DCD patients or three assays with carbachol alone (control) performed in triplicate. Mean values were compared using one-way ANOVA followed by a Bonferroni multicomparison test. (**A**) Significant differences: **** vs. Control ($p < 0.0001$); *** vs. Control ($p < 0.001$); #### vs. 0 min ($p < 0.0001$); &&&& vs. 15 min ($p < 0.0001$). Time 0 min corresponds to cells preincubated with a mixture of DCD IgG and carbachol. (**B**) A plot of ΔBRET vs. preincubation time, ranging from 0 to 60 min, yielded an exponential decay curve, indicating a good fit to a first-order decay model ($R^2 = 0.97$).

### *3.6. Inhibition of Agonist-Induced β-Arrestin Recruitment by $M_2$ Muscarinic Autoantibodies: Allosteric Mechanism*

To get more insight into the mechanism underlying the negative allosteric modulation of agonist-induced $M_2$R activation by anti-$M_2$R AAb, we assessed the effect of DCD IgG on the agonist's potency and efficacy in stimulating Arr-2 vs. Arr-3 recruitment. Thus, we performed BRET assays on HEKT/Arr-2 or HEKT/Arr-3 cells preincubated with buffer alone, DCD IgG, Control IgG, or gallamine, and further treated with carbachol at varying concentrations. Nonlinear regression analysis of agonist concentration–response (C-R) curves shows that preincubating cells with gallamine shifts the agonist curve to the right in both HEKT/Arr-2 and HEKT/Arr-3 cells, exhibiting higher $EC_{50}$ values without significant changes in $E_{max}$ values, as compared with control curves (KRHA buffer alone) (Figure 6A,B, Table 2). These decreases in agonist's potency are consistent with the well-

known pharmacodynamic behavior of gallamine as a NAM of agonist affinity. Control IgG does not promote significant changes in agonist-induced Arr-2 or Arr-3 recruitment. Thus, the Emax and $EC_{50}$ values are similar to those from control curves in both BRET cell systems. In HEK-Arr-2 cells, DCD IgG promotes a significant decrease in $E_{max}$ but not in $EC_{50}$. Such a noncompetitive inhibitory effect is typical of a negative allosteric ligand that can inhibit the efficacy of an agonist without modifying its potency. In contrast, DCD IgG promotes no changes in agonist-induced Arr-3 translocation in either potency or efficacy, which confirms the previous observation that anti-$M_2$R AAb cannot inhibit Arr-3 recruitment (Figure 3B).

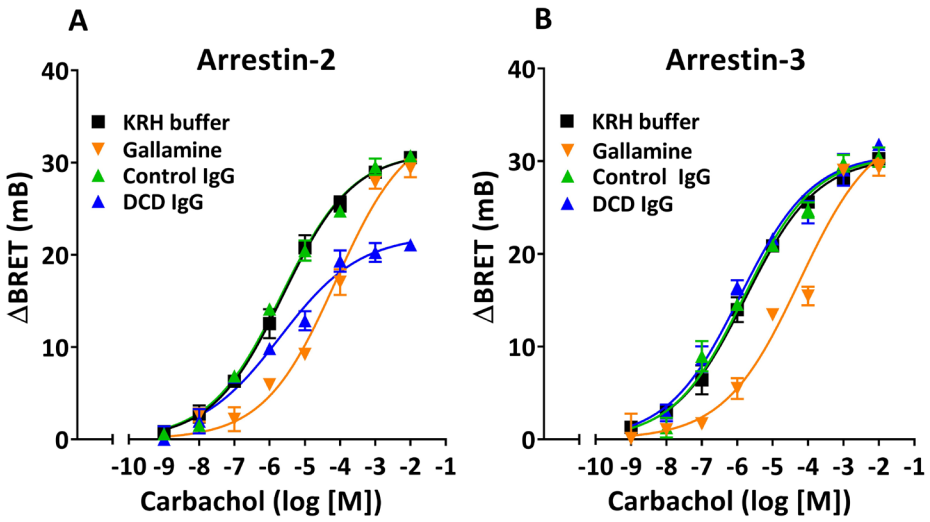



**Figure 6.** Inhibition of agonist-induced β-arrestin recruitment by anti-$M_2$R muscarinic antibodies from DCD patients. Characterization of the allosteric mechanism. HEKT/Arr-2 (**A**) or HEKT/Arr-3 (**B**) were preincubated in the presence or absence of 10 μM Control or DCD IgG for 30 min at 25 °C. Alternatively, cells were preincubated in the presence of 100 μM gallamine for 15 min at the same temperature. Following either approach, cells were treated with carbachol at various concentrations for an additional 20 min. Net changes in the BRET ratio were calculated as ΔBRET values and expressed in mB, as indicated in Figure 1. Data shown in (**A**,**B**) are the mean ± SEM of three independent experiments (buffer alone or gallamine) or three IgG fractions, performed at least in triplicate. All curves were best fit to a sigmoidal function using nonlinear regression analysis, which provided the pharmacodynamic parameters shown in Table 2.

**Table 2.** Allosteric inhibition of agonist-induced β-arrestin recruitment mediated by anti-$M_2$R autoantibodies from DCD patients. Pharmacodynamic parameters.

| | Arrestin-2 | | Arrestin-3 | |
|---|---|---|---|---|
| **Treatment** | **$pEC_{50}$** | **$E_{max}$ (mB)** | **$pEC_{50}$** | **$E_{max}$ (mB)** |
| KRHA Buffer | 5.63 ± 0.10 | 31.1 ± 0.8 | 5.77 ± 0.10 | 30.5 ± 0.8 |
| Gallamine | 4.13 ± 0.26 **** | 34.2 ± 3.0 | 4.24 ± 0.32 **** | 34.1 ± 3.5 |
| Control IgG | 5.67 ± 0.10 | 31.2 ± 0.8 | 5.81 ± 0.15 | 30.8 ± 1.2 |
| DCD IgG | 5.71 ± 0.22 | 22.1 ± 1.2 &&, &&&& | 5.92 ± 0.17 | 30.8 ± 1.3 |

Maximal effect ($E_{max}$) and negative log of the half-maximal effective concentration ($pEC_{50}$) values, as determined by nonlinear regression analyses of data shown in Figure 6A,B, are listed. Comparison of parameter values among curves within each panel (A or B) was made using one-way ANOVA followed by a Bonferroni multiple comparison test. Significant differences: **** vs. cells preincubated with buffer alone, Control IgG or DCD IgG ($p < 0.0001$); && vs. cells preincubated with either KRHA buffer or Control IgG ($p < 0.01$); &&&& vs. cells preincubated with gallamine ($p < 0.0001$).

## 4. Discussion

Evidence of a strong association between the presence of circulating anti-$M_2R$ antibodies and the presence of cardiovascular abnormalities and/or digestive disorders in *T. cruzi*-infected patients suggests that this antibody fraction could play a pathophysiological role in Chagas disease [29]. Over the years, several studies have demonstrated the intrinsic muscarinic activity of these autoantibodies in target organs associated with these disorders, such as the heart [5,9,12,13], esophagus [10], and colon [11] preparations, thereby supporting these hypotheses. Moreover, most studies on the pharmacological effects of muscarinic AAb to date have focused on their agonistic capacity, leading to the activation of Gi protein-mediated signal transduction pathways [9–11,30].

### *4.1. Intrinsic Activity of $M_2$ Muscarinic Receptor Autoantibodies*

In the present study, we examined whether these agonist-like anti-$M_2R$ AAb could enhance β-arrestin recruitment to the $M_2R$. The fact that DCD IgG does not stimulate the interaction between the $M_2R$ and Arr-2 or Arr-3 may have various implications: (a) The interaction between the $M_2R$ with specific AAb generates an active state in the receptor molecule that favors $G_i$ protein-activation but not β-arrestin translocation [5,15,24,30]. This suggests that $M_2$ muscarinic AAb act as biased ligands with intrinsic muscarinic activity towards $G_i$ protein signaling. (b) Given that agonist-induced $M_2R$ desensitization is mediated by β-arrestin recruitment to the phosphorylated receptor [31], the present findings are in agreement with previous data indicating that short-term exposure of $M_2R$ to serum anti-$M_2R$ AAb does not result in receptor desensitization [15,16,32]. (c) Because agonist-induced internalization of $M_2R$ can be arrestin-dependent [31,33], the present results are consistent with previous data demonstrating that anti-$M_2R$ AAb cannot promote $M_2R$ arrestin-dependent internalization [15,17].

### *4.2. Arr-2-Biased Modulation of β-Arrestin Recruitment by $M_2$ Muscarinic Receptor Autoantibodies*

The exposure of cellular $M_2R$ to anti-$M_2R$ AAb, followed by the addition of a muscarinic agonist, not only promotes a selective inhibition of Arr-2 recruitment but also the attenuation of $G_i$ activation [15]. This suggests that the AAb/$M_2R$ interaction promotes a conformational change in the receptor molecule, which results in an impaired active state upon agonist binding. The ternary AAb/$M_2R$/agonist complex does not promote $G_i$ protein activation or Arr-2 recruitment as efficiently as the binary agonist/$M_2R$ complex does. In contrast, the ternary complex does not hinder Arr-3 translocation, which occurs as efficiently as it would in the absence of AAb. This suggests that the inhibitory effect of AAb on β-arrestin recruitment is biased towards Arr-2.

### *4.3. $M_2$ Muscarinic Receptor Autoantibodies as Negative Allosteric Modulators*

The most critical finding in the present study is that the inhibitory effect of anti-$M_2R$ AAb from CD patients on Arr-2 recruitment is allosteric in nature: (a) The inhibitory activity of muscarinic AAb is neutralized by a synthetic peptide carrying the amino acid sequence of the II-ECL (Figure 4). Because the II-ECL is part of the allosteric binding site of the $M_2R$, these data indicate that anti-$M_2R$ AAb exert their inhibitory effect by interacting with the allosteric site of its target receptor. (b) The inhibition curve shows a partial inhibitory effect ($I_{max}$ < 100%), which reveals saturation of allosteric sites, and a Hill Slope less than -1, which reflects a negative cooperative effect [34]. These values are consistent with negative allosteric modulation (Figure 3A). (c) According to classical pharmacodynamics, NAM can promote a decrease in agonist affinity for the orthosteric site and/or a decrease in agonist efficacy [35]. These changes result in rightward and/or downward shifts in agonist concentration–response curves, respectively. Our carbachol curves in the presence of DCD

IgG indicate that the exposure of $M_2R$ to specific AAb, followed by agonist treatment, results in a decrease in agonist efficacy, but not in potency (Figure 6A and Table 2). As stated by Kenakin et al., when assay conditions provide a low receptor density (as in our BRET system), the chances of having a significant receptor reserve are negligible. In such a condition, a decrease in $E_{max}$ without an increase in $EC_{50}$ suggests a reduction in agonist efficacy, but not in affinity (noncompetitive effect) [35]. This conclusion is supported by the fact that anti-$M_2R$ AAb do not promote inhibition of Arr-3 recruitment to activated $M_2R$, since an otherwise hypothetical reduction in agonist's affinity generated by AAb should have also promoted a decrease in agonist potency, thereby shifting the agonist curve to the right (Figure 6B). Finally, the negative allosteric inhibition effect of anti-$M_2R$ AAb on agonist-induced receptor activation demonstrated in this study is also supported by previous results that had once proposed a partial agonistic activity for these AAb. In those studies, preincubation of rat atria with DCD IgG, its corresponding $F(ab')_2$ fraction, or monospecific anti-$M_2R$ IgG (anti-II-ECL) exerted non-competitive inhibition of agonist-induced negative inotropic effects in isolated heart assays [5,24,30].

### 4.4. Crosslinking-Mediated Negative Allosteric Modulation by $M_2R$ Autoantibodies

In a previous study, we reported that anti-$M_2R$ AAb from DCD patients could modestly enhance the BRET signal between $M_2R$-Rluc and $M_2R$-YFP in intact HEK 293T cells [20]. Given that the functional $M_2R$ in the cell membrane appears to be primarily a tetramer [36], the enhancing effect in BRET was interpreted as an antibody-induced conformational rearrangement within the $M_2R$ oligomer. The Fab fragment from DCD IgG was unable to mimic the effect of the bivalent AAb unless this bivalent structure was recreated in the presence of an anti-human Fab IgG antibody. These data suggest that anti-$M_2R$ AAb can crosslink adjacent receptors involved in preformed dimers or oligomers and stabilize pre-established $M_2$ receptor/receptor interactions. Years later, we found that these AAb could inhibit agonist-induced Arr-2 recruitment, and that this effect is mediated by receptor crosslinking [15]. Based on these results, we conclude that a crosslinking-mediated conformational rearrangement within the antibody-bound receptor oligomer results in an altered active state upon agonist binding, leading to an impairment of $M_2R$-associated signal transduction pathways. In other words, the negative allosteric modulation of agonist-induced $M_2R$ activation by anti-$M_2R$ AAb appears to be mediated by receptor crosslinking [37].

### 4.5. Time-Dependent Direction of Allosteric Modulation by $M_2$ Muscarinic Autoantibodies

When evaluating the effect of the exposure time of HEKT/Arr-2 cells to anti-$M_2R$ autoantibodies on agonist-induced Arr-2 recruitment, two modulatory effects—opposite in direction and different in rate and magnitude—were observed: (a) a rapid 45% enhancement of BRET resulting from a 20 min cell treatment with a combination of DCD IgG and carbachol added simultaneously; (b) an exponential decline in BRET that reaches a maximum 75% inhibition after cell preincubation with DCD IgG for 60 min and an additional 20 min incubation after addition of carbachol. Regarding the first approach (a), our results are consistent with data published by Hernandez et al., who reported that anti-$M_2R$ AAb can exert positive allosteric modulation of acetylcholine-induced negative chronotropism after 4 min incubation in an isolated rabbit heart preparation [17]. Interestingly, these authors show that AAb can potentiate the ACh response at agonist concentrations exceeding the $EC_{50}$, a finding similar to that observed in the present study. In contrast, the second approach (b) reveals a gradual inhibitory effect of AAb on agonist-induced Arr-2 recruitment, which requires a preincubation time of at least 30 min to become apparent. Considering all functional allosteric effects triggered by the IgG fraction from CD patients reported to date, we conclude that anti-$M_2R$ AAb can function as positive or negative

allosteric modulators of agonist-induced $M_2R$ activation. Through this mechanism, $M_2$ muscarinic AAb can either enhance or hinder the ability of the muscarinic agonist to promote $G_i$ protein activation and Arr-2 recruitment [15,17], depending on the timing of AAb application with respect to carbachol addition (simultaneously or before) and the duration of $M_2R$ exposure to AAb.

### *4.6. Implications of the Present Findings in the Pathophysiology and Therapeutics of Chagas Disease*

Anti-$M_2R$ AAb can bind to and activate cardiac $M_2R$, leading to $G_i$ protein activation, which can trigger negative inotropic and chronotropic effects [5,24,30]. However, in this report, we show that these AAb cannot stimulate Arr-2 or Arr-3 recruitment to the $M_2R$, which could otherwise promote short-term receptor regulation (desensitization of the AAb-mediated agonist-like response and/or internalization of the AAb-bound $M_2R$). This scenario generates an unregulated muscarinic response triggered by these AAb, which appears to play a pathogenic role in cardiac manifestations such as sinus node dysfunction [9] and genesis of the heterogeneity of ventricular repolarization and arrhythmia [12].

Negative allosteric modulation of $M_2R$ by $M_2$ muscarinic AAb is particularly relevant in the context of dysautonomia secondary to CD. In the chronic phase of *T. cruzi* infection, cardiac $M_2R$ undergoes sustained exposure to anti-$M_2R$ AAb. In this scenario, a significant population of $M_2R$ will form $M_2R$/AAb complexes. When ACh is released by cardiac parasympathetic nerve terminals, it will interact with AAb-bound $M_2R$ binary complexes. Upon ACh binding, the impaired active state in the ternary complexes would promote attenuated Gi protein activation (and Arr-2 recruitment), but unrestricted Arr-3 translocation. Therefore, a decreased efficacy of ACh in stimulating Gi protein signal transduction, combined with Arr-3-mediated $M_2R$ desensitization and internalization, would result in a reduction in ACh-induced negative chronotropic response, leading to parasympathetic dysautonomia.

Several strategies have been developed to counteract the detrimental effects of pathogenic AAb against GPCR. In particular, approaches aimed at disrupting the interaction between $M_2R$ and AAb, such as the use of synthetic peptides and aptamers, have proven effective in interfering with this interaction in both in vitro neutralization bioassays and in vivo preclinical mouse models [38–40]. The fact that conventional muscarinic allosteric ligands and functional AAb anti-$M_2R$ compete for binding to the same allosteric site within the target receptor suggests that the administration of muscarinic allosteric ligands could block the AAb/GPCR interaction, and thereby prevent AAb-mediated harmful effects [41]. For instance, Hernandez et al. have shown that the NAM gallamine can abolish the enhancement of ACh-induced negative chronotropic triggered by anti-$M_2R$ AAb on isolated rabbit hearts [17]. A few years later, Beltrame et al. demonstrated that gallamine can inhibit the enhancing effect of these AAb on $M_2$ muscarinic receptor/receptor interaction [20]. The enhanced interaction between two protomers involved in the $M_2$ muscarinic oligomer in the presence of anti-$M_2R$ AAb reflects the crosslinking-mediated conformational change in the receptor molecule, which results in the negative allosteric modulation of agonist-induced $M_2R$ activation [15]. In summary, these studies provide evidence suggesting that a muscarinic allosteric ligand, by interacting with the allosteric site of the $M_2R$, can block the binding of anti-$M_2R$ AAb and thereby attenuate both positive and negative allosteric effects exerted by these AAb.

The use of computational methods like molecular dynamics simulations and ligand docking to compare the interactions between the human $M_2R$ and monoclonal antibodies against cross-reacting *T. cruzi* antigens with those involving this receptor and muscarinic allosteric ligands could reveal new aspects of the pharmacological nature of $M_2R$/AAb interactions and the ability of muscarinic allosteric ligands to neutralize them [42–44].

Apart from Chagas disease, a large number of other medical conditions have been associated with the impaired autonomic control of cardiac or digestive function. Postural orthostatic tachycardia syndrome (POTS) is a particular type of dysautonomia characterized by an autonomic imbalance at the cardiovascular or digestive level (enhanced sympathetic activity and an attenuated vagal response) [45]. POTS can be classified as a primary (idiopathic) syndrome or secondary to a preexisting or coexisting infectious disease, like coronavirus disease 2019 (viral), Lyme disease (bacterial), and babesiosis (parasitic), among other medical conditions [46]. Interestingly, circulating functional antibodies interacting with autonomic neurotransmitter receptors, such as AAb to $\alpha_1$-adrenergic receptors (AAb anti-$\alpha_1$AR), AAb anti-$\beta_1$AR, and AAb anti-$M_2$R, have been identified in patients with POTS [47,48]. These AAb can moderately activate their target receptor and modulate agonist activity. However, while the AAb anti-$\beta_1$AR potentiates agonist activity, the AAb anti-$\alpha_1$AR and AAb anti-$M_2$R exert negative modulation. Therefore, the authors suggest that the former receptors could promote an increased sympathetic activity, while the latter may induce parasympathetic impairment [48]. Based on the present work, we encourage future studies involving AAb to GPCR from patients with various medical conditions to explore the potential allosteric nature of the modulatory activity exerted by these AAb. Binding studies as well as physiological and biochemical assays can be used to confirm that AAb exhibit true allosteric effects [17,37]. Moreover, other biochemical or immunocytochemical assays should rule out that the apparent allosteric activity of functional anti-GPCR AAb is merely the result of other regulatory mechanisms, such as receptor desensitization/internalization promoted by agonist-like AAb [15,17].

## 5. Conclusions

The present study demonstrates that serum anti-$M_2$R autoantibodies from patients with chronic Chagas disease do not stimulate the interaction between the $M_2$R and nonvisual arrestins (Arr-2 or Arr-3) in HEK 293T cells expressing $M_2$R. However, preincubation of these cells for at least 30 min with AAb and further treatment with carbachol results in a selective inhibition of Arr-2 translocation without modifying Arr-3 recruitment. Inhibition curves of carbachol-induced Arr-2 translocation by AAb show a submaximal effect and a Hill Slope deviation from unity. In addition, carbachol concentration–response assays exhibit a noncompetitive inhibitory effect on agonist-induced Arr-2 recruitment, but Arr-3 translocation remains unchanged. These data suggest that anti-$M_2$R AAb can function as NAM of agonist efficacy, and that their role as NAM of agonist-induced β-arrestin recruitment is biased towards arrestin-2. These AAb can also act as PAM when they act simultaneously with carbachol, which demonstrates that the direction of allosteric modulation depends on the timing of AAb application and the exposure time of $M_2$R to specific AAb.

**Supplementary Materials:** The following supporting information can be downloaded at https://www.mdpi.com/article/10.3390/cells14231857/s1. Minimal Dataset, Equations, Curve Fitting and Parameter Definitions.

**Author Contributions:** Conceptualization, L.C.C.P., S.P.B. and J.C.G.; methodology, L.C.C.P. and S.P.B.; validation, L.C.C.P., S.P.B. and J.C.G.; formal analysis, L.C.C.P., S.P.B., C.I.W. and J.C.G.; investigation, L.C.C.P., S.P.B., S.R.A., A.H.S., C.R.B., I.M.I., C.I.W. and J.C.G.; resources, S.R.A., A.H.S., C.R.B., I.M.I., C.I.W. and J.C.G.; data curation, L.C.C.P., S.P.B. and J.C.G.; writing—original draft preparation, L.C.C.P.; writing—review and editing, S.R.A., A.H.S., C.R.B., I.M.I., C.I.W. and J.C.G.; visualization L.C.C.P., S.P.B. and J.C.G.; supervision, J.C.G.; project administration, C.I.W.; funding acquisition, C.R.B., I.M.I., C.I.W. and J.C.G. All authors have read and agreed to the published version of the manuscript.

**Funding:** This research was funded by the National Council for Scientific and Technical Research (Argentina) with grant PIP CONICET 2023–2025 Nº 0433 to Juan C. Goin, and grant PIP CONICET 2023-2025 Nº 0027 to Isabel M. Irurzun.

**Institutional Review Board Statement:** The investigations reported in the present article were conducted following the rules of the Declaration of Helsinki of 1975, which was revised in 2013. Accordingly, the research protocols involved in this study were approved by the Directive Council of the School of Medicine, University of Buenos Aires (UBA), by resolution Nº RESCD-2023-873-E-UBA-DCT#FMED dated 12 May 2023, following the recommendation from the Research Commission and the Human Ethics Committee of this Institution.

**Informed Consent Statement:** Informed consent was obtained from all subjects involved in the study.

**Data Availability Statement:** The datasets generated and/or analyzed during the current study are available from the corresponding author upon reasonable request. The minimal dataset is included in the Supplementary Materials.

**Acknowledgments:** We would like to thank Patricia M. Fernández, M. Alejandra Verón, M. Cristina Lincon, Daniela C. Néspola, Alcira Mazziotti, Vanesa Fernández, Rosana Leiva, and Daniel Guerrero from the CEFYBO Institute for their technical assistance. We would also like to thank Santiago Lamuedra, Tamara S. Agra Skoropada, and Leandro Sarmiento for their assistance in setting up BRET-based experiments. We are also grateful to Valeria Barrera, Pablo Gallinotti, and Silvia Palacios for their invaluable help in collecting blood samples for this research project.

**Conflicts of Interest:** The authors declare no conflicts of interest.

## Abbreviations

The following abbreviations are used in this manuscript:

| | |
|---|---|
| II-ECL | second extracellular loop |
| $\alpha_1$AR | $\alpha_1$ adrenergic receptor |
| βAR, $\beta_1$AR, or $\beta_2$AR | β, $\beta_1$, or $\beta_2$ adrenergic receptor(s) |
| AAb | autoantibody(ies) |
| ACh | acetylcholine |
| Anti-$\alpha_1$AR AAb | AAb against $\alpha_1$AR |
| Anti-βAR AAb, anti-$\beta_1$AR AAb, or anti-$\beta_2$AR AAb | AAb against βAR, $\beta_1$AR, or $\beta_2$AR |
| Anti-$M_2$R AAb/$M_2$R AAb | AAb against $M_2$R |
| Arr-2 or Arr-3 | arrestin-2 or arrestin-3 |
| Arr-2-YFP or Arr-3-YFP | Arr-2 or Arr-3 fused to enhanced yellow fluorescence protein |
| BRET | bioluminescence resonance energy transfer |
| BSA | bovine serum albumin |
| CD | Chagas disease |
| C-R | concentration–response |
| Control IgG | IgG(s) from (a) noninfected individual(s) |
| DCD IgG | IgG(s) from (a) patient(s) with DCD |
| DCD | dysautonomia secondary to CD |
| ECG | electrocardiogram |
| ERI | ELISA reactivity index |
| FBS | fetal bovine serum |
| GPCR | G protein-coupled receptor |
| GRK2 | G protein-coupled receptor kinase 2 |
| KHRA | Krebs-HEPES-Ringer buffer supplemented with BSA |
| $M_2$R | $M_2$ muscarinic receptor(s) |
| $M_2$R-RLuc | $M_2$R fused to *Renilla* luciferase |
| NAM | negative allosteric modulator(s) |

| | |
|---|---|
| PAM | positive allosteric modulator(s) |
| PBS | phosphate-buffered saline |
| POTS | postural orthostatic tachycardia syndrome |
| RFU | relative fluorescence units |
| RLU | relative luminescence units |
| SD | standard deviation |
| *T. cruzi* | *Trypanosoma cruzi* |

## References


1. Cucunuba, Z.M.; Gutierrez-Romero, S.A.; Ramirez, J.D.; Velasquez-Ortiz, N.; Ceccarelli, S.; Parra-Henao, G.; Henao-Martinez, A.F.; Rabinovich, J.; Basanez, M.G.; Nouvellet, P.; et al. The epidemiology of Chagas disease in the Americas. *Lancet Reg. Health Am.* **2024**, *37*, 100881. [CrossRef] [PubMed]
2. Nunes, M.C.P.; Beaton, A.; Acquatella, H.; Bern, C.; Bolger, A.F.; Echeverria, L.E.; Dutra, W.O.; Gascon, J.; Morillo, C.A.; Oliveira-Filho, J.; et al. Chagas Cardiomyopathy: An Update of Current Clinical Knowledge and Management: A Scientific Statement From the American Heart Association. *Circulation* **2018**, *138*, e169–e209. [CrossRef] [PubMed]
3. Borda, E.; Pascual, J.; Cossio, P.; De La Vega, M.; Arana, R.; Sterin-Borda, L. A circulating IgG in Chagas' disease which binds to beta-adrenoceptors of myocardium and modulates their activity. *Clin. Exp. Immunol.* **1984**, *57*, 679–686.
4. Sterin-Borda, L.; Perez Leiros, C.; Wald, M.; Cremaschi, G.; Borda, E. Antibodies to beta 1 and beta 2 adrenoreceptors in Chagas' disease. *Clin. Exp. Immunol.* **1988**, *74*, 349–354. [PubMed]
5. Goin, J.C.; Borda, E.; Leiros, C.P.; Storino, R.; Sterin-Borda, L. Identification of antibodies with muscarinic cholinergic activity in human Chagas' disease: Pathological implications. *J. Auton. Nerv. Syst.* **1994**, *47*, 45–52. [CrossRef]
6. Ferrari, I.; Levin, M.J.; Wallukat, G.; Elies, R.; Lebesgue, D.; Chiale, P.; Elizari, M.; Rosenbaum, M.; Hoebeke, J. Molecular mimicry between the immunodominant ribosomal protein P0 of *Trypanosoma cruzi* and a functional epitope on the human beta 1-adrenergic receptor. *J. Exp. Med.* **1995**, *182*, 59–65. [CrossRef]
7. Elies, R.; Ferrari, I.; Wallukat, G.; Lebesgue, D.; Chiale, P.; Elizari, M.; Rosenbaum, M.; Hoebeke, J.; Levin, M.J. Structural and functional analysis of the B cell epitopes recognized by anti-receptor autoantibodies in patients with Chagas' disease. *J. Immunol.* **1996**, *157*, 4203–4211. [CrossRef]
8. Mahler, E.; Hoebeke, J.; Levin, M.J. Structural and functional complexity of the humoral response against the *Trypanosoma cruzi* ribosomal P2 beta protein in patients with chronic Chagas' heart disease. *Clin. Exp. Immunol.* **2004**, *136*, 527–534. [CrossRef]
9. Chiale, P.A.; Ferrari, I.; Mahler, E.; Vallazza, M.A.; Elizari, M.V.; Rosenbaum, M.B.; Levin, M.J. Differential profile and biochemical effects of antiautonomic membrane receptor antibodies in ventricular arrhythmias and sinus node dysfunction. *Circulation* **2001**, *103*, 1765–1771. [CrossRef]
10. Goin, J.C.; Sterin-Borda, L.; Bilder, C.R.; Varrica, L.M.; Iantorno, G.; Rios, M.C.; Borda, E. Functional implications of circulating muscarinic cholinergic receptor autoantibodies in chagasic patients with achalasia. *Gastroenterology* **1999**, *117*, 798–805. [CrossRef]
11. Sterin-Borda, L.; Goin, J.C.; Bilder, C.R.; Iantorno, G.; Hernando, A.C.; Borda, E. Interaction of human chagasic IgG with human colon muscarinic acetylcholine receptor: Molecular and functional evidence. *Gut* **2001**, *49*, 699–705. [CrossRef]
12. Medei, E.; Pedrosa, R.C.; Benchimol Barbosa, P.R.; Costa, P.C.; Hernandez, C.C.; Chaves, E.A.; Linhares, V.; Masuda, M.O.; Nascimento, J.H.; Campos de Carvalho, A.C. Human antibodies with muscarinic activity modulate ventricular repolarization: Basis for electrical disturbance. *Int. J. Cardiol.* **2007**, *115*, 373–380. [CrossRef]
13. Goin, J.C.; Borda, E.S.; Auger, S.; Storino, R.; Sterin-Borda, L. Cardiac M(2) muscarinic cholinoceptor activation by human chagasic autoantibodies: Association with bradycardia. *Heart* **1999**, *82*, 273–278. [CrossRef]
14. Ribeiro, A.L.; Gimenez, L.E.; Hernandez, C.C.; de Carvalho, A.C.; Teixeira, M.M.; Guedes, V.C.; Barros, M.V.; Lombardi, F.; Rocha, M.O. Early occurrence of anti-muscarinic autoantibodies and abnormal vagal modulation in Chagas disease. *Int. J. Cardiol.* **2007**, *117*, 59–63. [CrossRef]
15. Beltrame, S.P.; Carrera Paez, L.C.; Auger, S.R.; Sabra, A.H.; Bilder, C.R.; Waldner, C.I.; Goin, J.C. Impairment of agonist-induced M2 muscarinic receptor activation by autoantibodies from chagasic patients with cardiovascular dysautonomia. *Clin. Immunol.* **2020**, *212*, 108346. [CrossRef] [PubMed]
16. de Oliveira, S.F.; Pedrosa, R.C.; Nascimento, J.H.; Campos de Carvalho, A.C.; Masuda, M.O. Sera from chronic chagasic patients with complex cardiac arrhythmias depress electrogenesis and conduction in isolated rabbit hearts. *Circulation* **1997**, *96*, 2031–2037. [CrossRef] [PubMed]
17. Hernandez, C.C.; Nascimento, J.H.; Chaves, E.A.; Costa, P.C.; Masuda, M.O.; Kurtenbach, E.; Campos, D.E.C.A.C.; Gimenez, L.E. Autoantibodies enhance agonist action and binding to cardiac muscarinic receptors in chronic Chagas' disease. *J. Recept. Signal Transduct. Res.* **2008**, *28*, 375–401. [CrossRef] [PubMed]

18. Leppik, R.A.; Miller, R.C.; Eck, M.; Paquet, J.L. Role of acidic amino acids in the allosteric modulation by gallamine of antagonist binding at the m2 muscarinic acetylcholine receptor. *Mol. Pharmacol.* **1994**, *45*, 983–990. [CrossRef]
19. Hernandez, C.C.; Barcellos, L.C.; Gimenez, L.E.; Cabarcas, R.A.; Garcia, S.; Pedrosa, R.C.; Nascimento, J.H.; Kurtenbach, E.; Masuda, M.O.; Campos de Carvalho, A.C. Human chagasic IgGs bind to cardiac muscarinic receptors and impair L-type $Ca^{2+}$ currents. *Cardiovasc. Res.* **2003**, *58*, 55–65. [CrossRef]
20. Beltrame, S.P.; Auger, S.R.; Bilder, C.R.; Waldner, C.I.; Goin, J.C. Modulation of M(2) muscarinic receptor-receptor interaction by immunoglobulin G antibodies from Chagas' disease patients. *Clin. Exp. Immunol.* **2011**, *164*, 170–179. [CrossRef]
21. Pan American Health Organization. *Guidelines for the Diagnosis and Treatment of Chagas Disease*; PAHO: Washington, DC, USA, 2019. Available online: https://iris.paho.org/bitstream/handle/10665.2/49653/9789275120439_eng.pdf (accessed on 18 November 2025).
22. Iosa, D.; Dequattro, V.; Lee, D.D.; Elkayam, U.; Caeiro, T.; Palmero, H. Pathogenesis of cardiac neuro-myopathy in Chagas' disease and the role of the autonomic nervous system. *J. Auton. Nerv. Syst.* **1990**, *30*, S83–S87. [CrossRef] [PubMed]
23. Ziegler, D.; Laux, G.; Dannehl, K.; Spuler, M.; Muhlen, H.; Mayer, P.; Gries, F.A. Assessment of cardiovascular autonomic function: Age-related normal ranges and reproducibility of spectral analysis, vector analysis, and standard tests of heart rate variation and blood pressure responses. *Diabet. Med.* **1992**, *9*, 166–175. [CrossRef] [PubMed]
24. Goin, J.C.; Leiros, C.P.; Borda, E.; Sterin-Borda, L. Interaction of human chagasic IgG with the second extracellular loop of the human heart muscarinic acetylcholine receptor: Functional and pathological implications. *FASEB J.* **1997**, *11*, 77–83. [CrossRef] [PubMed]
25. Fu, L.X.; Magnusson, Y.; Bergh, C.H.; Liljeqvist, J.A.; Waagstein, F.; Hjalmarson, A.; Hoebeke, J. Localization of a functional autoimmune epitope on the muscarinic acetylcholine receptor-2 in patients with idiopathic dilated cardiomyopathy. *J. Clin. Investig.* **1993**, *91*, 1964–1968. [CrossRef]
26. Lowry, O.H.; Rosebrough, N.J.; Farr, A.L.; Randall, R.J. Protein measurement with the Folin phenol reagent. *J. Biol. Chem.* **1951**, *193*, 265–275. [CrossRef]
27. Mellon, P.; Parker, V.; Gluzman, Y.; Maniatis, T. Identification of DNA sequences required for transcription of the human alpha 1-globin gene in a new SV40 host-vector system. *Cell* **1981**, *27*, 279–288. [CrossRef]
28. Carrera Páez, L.C. Interacción del Receptor Muscarínico M2 con Arrestinas no Visuales y su Modulación por Anticuerpos Séricos de Pacientes Chagásicos Crónicos. Master's Thesis, Universidad de Buenos Aires, Facultad de Farmacia y Bioquímica, Buenos Aires, Argentina, 13 October 2021. Available online: http://repositoriouba.sisbi.uba.ar/gsdl/cgi-bin/library.cgi?a=d&c=afamaster&cl=CL1&d=HWA_7958 (accessed on 18 November 2025).
29. Herda, L.R.; Felix, S.B.; Boege, F. Drug-like actions of autoantibodies against receptors of the autonomous nervous system and their impact on human heart function. *Br. J. Pharmacol.* **2012**, *166*, 847–857. [CrossRef]
30. Goin, J.C.; Perez Leiros, C.; Borda, E.; Sterin-Borda, L. Modification of cholinergic-mediated cellular transmembrane signals by the interaction of human chagasic IgG with cardiac muscarinic receptors. *Neuroimmunomodulation* **1994**, *1*, 284–291. [CrossRef]
31. Pals-Rylaarsdam, R.; Gurevich, V.V.; Lee, K.B.; Ptasienski, J.A.; Benovic, J.L.; Hosey, M.M. Internalization of the m2 muscarinic acetylcholine receptor. Arrestin-independent and -dependent pathways. *J. Biol. Chem.* **1997**, *272*, 23682–23689. [CrossRef]
32. Wallukat, G.; Fu, H.M.; Matsui, S.; Hjalmarson, A.; Fu, M.L. Autoantibodies against M2 muscarinic receptors in patients with cardiomyopathy display non-desensitized agonist-like effects. *Life Sci.* **1999**, *64*, 465–469. [CrossRef]
33. Jones, K.T.; Echeverry, M.; Mosser, V.A.; Gates, A.; Jackson, D.A. Agonist mediated internalization of M2 mAChR is beta-arrestin-dependent. *J. Mol. Signal.* **2006**, *1*, 7. [CrossRef] [PubMed]
34. Silvano, E.; Millan, M.J.; Mannoury la Cour, C.; Han, Y.; Duan, L.; Griffin, S.A.; Luedtke, R.R.; Aloisi, G.; Rossi, M.; Zazzeroni, F.; et al. The tetrahydroisoquinoline derivative SB269,652 is an allosteric antagonist at dopamine D3 and D2 receptors. *Mol. Pharmacol.* **2010**, *78*, 925–934. [CrossRef] [PubMed]
35. Kenakin, T.P. Allosteric Modulation. In *A Pharmacology Primer: Techniques for More Effective and Strategic Drug Discovery*, 5th ed.; Elsevier/Academic Press: London, UK, 2019; pp. 173–205.
36. Pisterzi, L.F.; Jansma, D.B.; Georgiou, J.; Woodside, M.J.; Chou, J.T.; Angers, S.; Raicu, V.; Wells, J.W. Oligomeric size of the m2 muscarinic receptor in live cells as determined by quantitative fluorescence resonance energy transfer. *J. Biol. Chem.* **2010**, *285*, 16723–16738. [CrossRef] [PubMed]
37. Skiba, M.A.; Kruse, A.C. Autoantibodies as Endogenous Modulators of GPCR Signaling. *Trends Pharmacol. Sci.* **2021**, *42*, 135–150. [CrossRef]
38. Sterin-Borda, L.; Joensen, L.; Bayo-Hanza, C.; Esteva, M.; Borda, E. Therapeutic use of muscarinic acetylcholine receptor peptide to prevent mice chagasic cardiac dysfunction. *J. Mol. Cell. Cardiol.* **2002**, *34*, 1645–1654. [CrossRef]
39. Wallukat, G.; Muller, J.; Haberland, A.; Berg, S.; Schulz, A.; Freyse, E.J.; Vetter, R.; Salzsieder, E.; Kreutz, R.; Schimke, I. Aptamer BC007 for neutralization of pathogenic autoantibodies directed against G-protein coupled receptors: A vision of future treatment of patients with cardiomyopathies and positivity for those autoantibodies. *Atherosclerosis* **2016**, *244*, 44–47. [CrossRef]

40. Haberland, A.; Holtzhauer, M.; Schlichtiger, A.; Bartel, S.; Schimke, I.; Muller, J.; Dandel, M.; Luppa, P.B.; Wallukat, G. Aptamer BC 007—A broad spectrum neutralizer of pathogenic autoantibodies against G-protein-coupled receptors. *Eur. J. Pharmacol.* **2016**, *789*, 37–45. [CrossRef]
41. Singh, K.D.; Jara, Z.P.; Harford, T.; Saha, P.P.; Pardhi, T.R.; Desnoyer, R.; Karnik, S.S. Novel allosteric ligands of the angiotensin receptor AT1R as autoantibody blockers. *Proc. Natl. Acad. Sci. USA* **2021**, *118*, e2019126118. [CrossRef]
42. Smulski, C.; Labovsky, V.; Levy, G.; Hontebeyrie, M.; Hoebeke, J.; Levin, M.J. Structural basis of the cross-reaction between an antibody to the *Trypanosoma cruzi* ribosomal P2beta protein and the human beta1 adrenergic receptor. *FASEB J.* **2006**, *20*, 1396–1406. [CrossRef]
43. Pizarro, J.C.; Boulot, G.; Bentley, G.A.; Gomez, K.A.; Hoebeke, J.; Hontebeyrie, M.; Levin, M.J.; Smulski, C.R. Crystal structure of the complex mAb 17.2 and the C-terminal region of *Trypanosoma cruzi* P2beta protein: Implications in cross-reactivity. *PLoS Negl. Trop. Dis.* **2011**, *5*, e1375. [CrossRef]
44. Korczynska, M.; Clark, M.J.; Valant, C.; Xu, J.; Moo, E.V.; Albold, S.; Weiss, D.R.; Torosyan, H.; Huang, W.; Kruse, A.C.; et al. Structure-based discovery of selective positive allosteric modulators of antagonists for the M2 muscarinic acetylcholine receptor. *Proc. Natl. Acad. Sci. USA* **2018**, *115*, E2419–E2428. [CrossRef]
45. Chakraborty, P.; Farhat, K.; Morris, L.; Whyte, S.; Yu, X.; Stavrakis, S. Non-invasive Vagus Nerve Simulation in Postural Orthostatic Tachycardia Syndrome. *Arrhythm. Electrophysiol. Rev.* **2023**, *12*, e31. [CrossRef]
46. Adler, B.L.; Chung, T.; Rowe, P.C.; Aucott, J. Dysautonomia following Lyme disease: A key component of post-treatment Lyme disease syndrome? *Front. Neurol.* **2024**, *15*, 1344862. [CrossRef]
47. Li, H.; Yu, X.; Liles, C.; Khan, M.; Vanderlinde-Wood, M.; Galloway, A.; Zillner, C.; Benbrook, A.; Reim, S.; Collier, D.; et al. Autoimmune basis for postural tachycardia syndrome. *J. Am. Heart Assoc.* **2014**, *3*, e000755. [CrossRef]
48. Li, H.; Zhang, G.; Forsythe, E.; Okamoto, L.E.; Yu, X. Implications of Antimuscarinic Autoantibodies in Postural Tachycardia Syndrome. *J. Cardiovasc. Transl. Res.* **2022**, *15*, 438–440. [CrossRef] [PubMed]


**Disclaimer/Publisher's Note:** The statements, opinions and data contained in all publications are solely those of the individual author(s) and contributor(s) and not of MDPI and/or the editor(s). MDPI and/or the editor(s) disclaim responsibility for any injury to people or property resulting from any ideas, methods, instructions or products referred to in the content.